Third International Conference on Sustainable Construction Materials and Technologies http://www.claisse.info/Proceedings.htm

Mechanical Properties of Prestressed Ultra High Strength Concrete beam with a Molten Slag as Fine Aggregate

H., Asai[1], S.,Ohta[2], R., Sato[3] and M., Suzuki[4]

[1] *Sumitomo Mitsui Construction Co., Ltd, Japan, 518-1, Komaki, Nagareyama-Shi, Chiba, 270-0132, h-asai@smcon.co.jp*
[2] *Ministry of Defence, Chugoku-Shikoku Defence Bureau, Japan,6-30, Kami-hacchobori, Naka-ku, Hiroshima-Shi, Hiroshima, 730-0012, s-ohta@chushi.rdb.mod.go.jp*
[3] *Graduate School of Engineering, Hiroshima University, Japan, 1-4--1,Kagamiyama, Higashi-Hiroshima-Shi, Hiroshima, sator@hiroshima-u.co.jp*
[4] *P. S. Mitsubishi Construction Co., Ltd, Japan, 2-1-67,Minami-kamonomiya, Odawara-Shi, Kanagawa, 250-0875, msuzuki@psmic.co.jp*

ABSTRACT

The present study aims at investigating the applicability of a molten slag (MS) as a fine aggregate to not only ultra high strength concrete (UHSC) but also prestressed concrete beam made of UHSC. Water-cement ratio of the present concrete and replacement ratio of the MS were 0.17 and 30 % in volume, respectively. Two beams with and without the MS both of which were 0.2m wide, 1.05m high and 8.8m long, were prepared to investigate the effect of the MS on mechanical properties of the concrete and prestressed concrete beams. The test results showed that strength and Young's modulus of concrete with MS were almost the same as those without MS, structural performance such as prestress loss, deflection and ultimate capacities of both beam were also almost the same, and the MS is applicable to UHSC as a fine aggregate from structural performance point of view.

Keywords. Molten Slag, Ultra High Strength Concrete, Prestressed Concrete, Mechanical properties

INTRODUCTION

A molten slag (MS) is produced by melting ash incinerated municipal waste at the temperature of 1200 ºC or more and subsequently by cooling down and granulating the molten ash by water. It is expected to apply the MS as a fine aggregate to various types of concrete structures in order to reduce the environmental impact as well as disposal cost as much as possible. From this background, JIS A 5031 was established in order to utilize the molten slag as a fine aggregate for concrete. However, utilization to ready mixed concrete was prohibited in 2010, because the pop-out occurred in reinforced concrete buildings due to use of non-JIS molten slag. Utilization to prestressed concrete was also prohibited at the same time. However, if the test method to guarantee the quality requirement of MS is established, this standard may be withdrawn and the MS may be utilized to various types of concrete structures. The present study aims at investigating the applicability of MS as a fine

aggregate to not only ultra high strength concrete (UHSC) but also prestressed concrete beam made of UHSC in order to prolong the life of concrete structures subjected to chloride attack as well as reduce the self-weight of superstructures in addition to the above-mentioned expectation for the reduction of environmental impact and disposal expense.

OUTLINE OF EXPERIMENT

Materials and Mixture. Table 1 gives the physical properties of the materials used in the PC beams. Cement is low-heat cement (SFLC) which is premixed by 10.4% with silica fume. Lime stone-crushed sand and molten slag-granulated sand were used as a fine aggregate and diabase-crushed gravel were used as a coarse aggregate. The molten slag-fine aggregate (MS) is produced by melting ash incinerated municipal waste at the temperature of 1300 ºC in arc-type melting furnace and subsequently by cooling down and granulating the molten ash by water. As a chemical admixture, polycarboxylate acid based high-range water reducing agent was used. Prestressing steel used was prestressing strand designated as SWPR7BLφ15.2 in JIS which was 1600N/mm^2 in yield strength and 1881N/mm^2 in ultimate strength. Two types of concretes were prepared which were reference UHSC not containing MS (Ref.-U) and UHSC containing MS (MS-U), respectively, as shown in Table 2. The fine aggregate of MS-U was replaced 30% in volume with the MS. In each mixture, the water-to-binder ratio (W/SFLC) was set to 0.17. The bulk volume of fine aggregate per unit volume of concrete was determined as 0.53m^3/m^3 to meet workability requirement. The slump flow was set to 675±75mm by adjusting quantity of the superplasticizer.

Table 1. Properties of Materials

Materials	Type	Properties	Notation
Cement	Low-heat cement	Density : 3.22g/cm^3, Specific surface area : 3590cm^2/g	LC
Silicafume		Density : 2.25g/cm^3, Specific surface area : 19.9m^2/g	SF
Silicafume Cement	Premixed	SF/(SF+LC)=0.104, Dencity : 3.08g/cm^3 Specific surface area : 6390cm^2/g	SFLC
Fine aggregate	Crushed sand	Surface-dry density : 2.65g/cm^2, Water absorption : 1.31% Fineness modulus : 2.74, Solid volume percentage : 68.2%	S
	Molten slag	Surface-dry density : 2.78g/cm^2, Water absorption : 0.47% Fineness modulus : 2.97, Solid volume percentage : 61.8%	MS
Coarse Aggregate	Crushed gravel	Surface-dry density : 2.92g/cm^2, Water absorption : 0.45% Fineness modulus : 6.50, Solid volume percentage : 59.1%	G
Chemical admixture	High-range water reducing agent super plasticizer	Aminopoly carboxylate	SP

Table 2. Mixture Proportions of Concrete

Mixture designation	W/SFLC (%)	Unit content (kg/m^3)					
		W	SFLC	S	MS	G	SP
Mix-Base	17	155	912	572	0	914	10.9
Mix-MS	17	155	912	400	181	914	10.9

Specimens. Two pre-tensioned PC beams made of UHSC not containing MS (Ref.-U) and containing MS (MS-U) were prepared. Dimension and configuration of beams are shown in Figure 1. As is shown in the figure, the beams were 0.2m wide, 1.05m high and 8.8m long.

Eight PC strands of 15.2mm in diameter were arranged on the bottom side of a beam section, and three PC strands were arranged on the top side. The prestressing strand ratio on bottom side was 0.0058 for full section. No shear reinforcement was arranged in the test zone with the length of 6300 mm. The prestressing stress before placing concrete was 1307N/mm^2 which was about 70 % of the technical standard tensile strength (1881N/mm^2) of the strand. The upper surface of Ref.-U was covered by waterproof sheets for two days. The upper surface of MS-U was covered by the plastic wrap to control evaporation of water as much as possible. Five hours later, the upper surface of the beam was covered with the curing mat and sheet. Forty eight hours later, the forms of both beams were removed the prestressing strands were slowly released. The end surfaces of beams were sealed by aluminium adhesive tapes so that the drying shrinkage could develop uniformly in the longitudinal direction. Cylindrical specimens with the diameter of 100mm and height of 200mm for test of compression strength and Young's modulus as well as those with the diameter of 150mm and height of 200mm for test of splitting tensile strength were also made, which were cured under the same condition as PC beams. Test specimens for fracture energy were made in accordance with test method of Japan Concrete Institute (JCI 2001) which was 100mm x 100mm x 400mm. The curing method of the specimens is the same as that of the above-mentioned specimens.

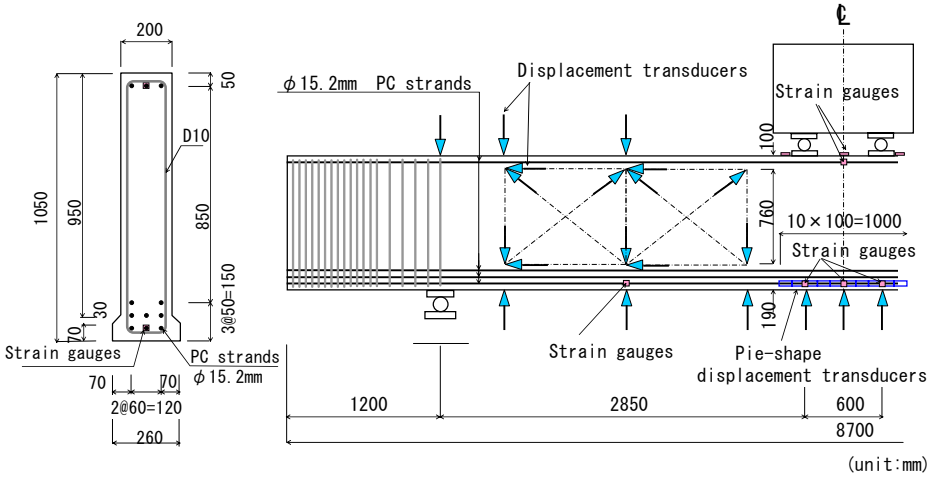

Figure 1. Detail of PC beam and location of LVDTs

Test Method. As is shown in Figure 1, the PC beams with the span of 6.3m were loaded symmetrically with two concentrated loads. The constant moment zone length and the shear span-to-effective depth ratio (a/d) were 0.6m and 2.98, respectively. The beams were loaded in the first step until the flexural crack reached the depth of the lowest PC strand. After that the beams were unloaded and subsequently the π shaped displacement transducer with measuring length of 100mm was installed to estimate prestress in concrete by measuring bending moment at crack opening on the bottom. In the second step, the beams were loaded up to failure. The deflections of the beams were measured with linear variable differential transducers (LVDTs) with the capacities from 25mm to 100mm, and minimum graduations from 0.002mm to 0.01mm at the span center, both supports and both loading points. Eleven LVDTs were installed on the side face in shear span of the beam to obtain shear displacement and principal displacements together with those principal directions. The strains of PC strands were measured by wire strain gauges with the length of 2mm. The concrete compressive strain was measured by wire strain gauge with the length of 60mm on the top surface at the span center section. The crack widths were measured using ten π

shaped displacement transducers similar to the above-mentioned transducers which were installed to the side surface at the depth of lowest strand. Figure 1 illustrates the locations of the strain gauges, LVDTs, and π shaped transducers. Strains and displacements measured by these transducers and strain gauges were recorded by an automatic data-logging system. Compressive and splitting tensile strength test was performed in accordance with JIS A 1113 and Young's modulus was obtained by measuring compression strain with JIS A 1149. Fracture energy test was conducted in accordance with test method of JCI (2001). Specimens were gaped at center section by a diamond cutter. The gap is 4mm in width and 50mm in depth. Specimens were loaded by displacement controlled loading machine with the capacity of 100 kN. Crack mouth opening displacement (CMOD) was measured by π shaped displacement transducer with the minimum graduation of 0.001 mm. Loading was conducted at the age of beam test.

RESULTS AND DISCUSSION

Material Characteristics. Control specimens were cast in 100mm diameter and 200mm high cylinders and cured simultaneously with the PC beam to determine the compressive strength f_c and splitting tensile strength f_t. Figure 2 shows the compressive strength of Ref.-U and MS-U. The compressive strength of Ref.-U developed with age almost similarly to that of MS-U and not only Ref.-U but also MS-U reached 150N/mm^2 at the age of 180 days, which implied that MS was applicable to UHSC as a fine aggregate with regard to compressive strength development. The regression curve of relationship between compressive strength and age was given by Eq.(1).

$$f_c(t_e) = 132\exp[0.250\{1-(28/t_e)^{0.5}\}] \quad (1)$$

where t_e is a temperature adjusted age (days) of concrete. It can be expressed as

$$t_e = \sum_{i=1}^{n} t_i[\exp\ 13.65 + \frac{4000}{273 + T(\Delta t_i)/T_0}\ ] \quad (2)$$

where Δt_i is the number of days when the temperature is T; T_0 is 1 degree; and $f_c(t)$ is the compressive strength in t_e days.

Figure 3 gives the relationships between Young's modulus and the compressive strength of the both UHSC. PCEA guideline (2008) recommends Eq.(3) to obtain Young's modulus ($E_{PCEA}(t_e)$) in compression using the compression strength for concrete with the compressive strength exceeding 60N/mm^2. In this study, Young's modulus in t days ($E_c(t_e)$) is basically given by Eq.(4) independent of replacement or non-replacement of the MS. According to this equation, Young's modulus of the both UHSC is approximately 52kN/mm^2 when the compressive strength is 150N/mm^2, which is 19 % higher than that obtained from PCEA Guidelines (2008) equation. It is thought that this difference is attributed to hardness of the course aggregate.

$$E_{PCEA}(t_e) = 12.5 f_c(t_e)^{1/4} \quad (3)$$

$$E_c(t_e) = 5.94 f_c(t_e)^{0.438} \quad (4)$$

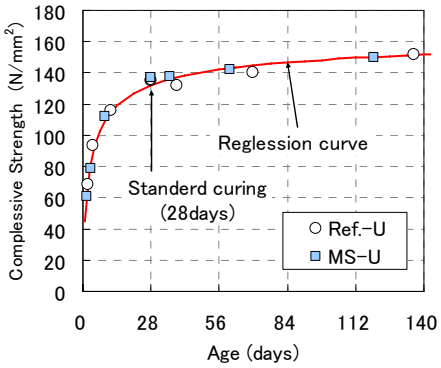

Figure 2. Compressive strength with time

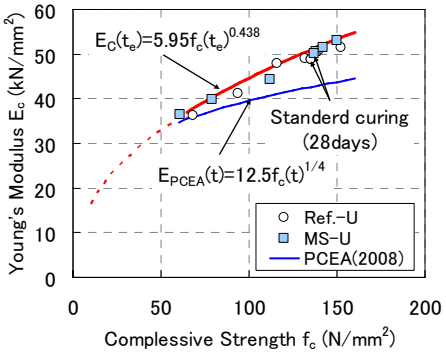

Figure 3. Comparison of compressive strength and Young's Modulus

Figure 4 shows the relation between the splitting tensile strength and the compressive strength. The splitting tensile strength of MS-U developed approximately similarly to that of Ref.-U without two noticeably small values of Ref.-U between 100N/mm^2 and 150 N/mm^2 in compression strength, while the former was 13 % smaller than the latter at the loading test of PC beams. The concrete properties at the loading test of the beams are summarized in Table 3. According to the table, the compressive strength and Young's modulus of MS-U are the same as those of Ref.-U, but the splitting tensile strength and fracture energy of MS-U are smaller and slightly smaller than those of Ref.-U, respectively. The reason for the latter may be due to the low bond strength between mortar and MS.

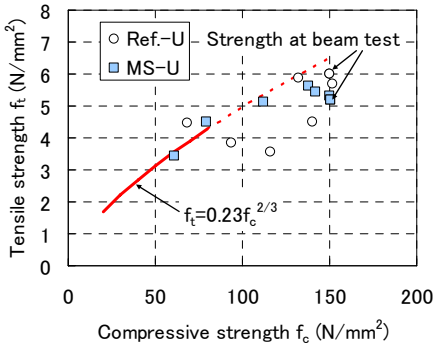

Figure 4. Comparison of compressive strength and tensile strength

Table 3. Concrete properties at the beam test

Properties		Ref.-U	MS-U
Compressive strength	f_c (N/mm^2)	150.0	150.6
Young's modulus	E_c (kN/mm^2)	51.0	51.0
Tensile strength	f_t (N/mm^2)	6.0	5.2
Fracture energy	G_F (N/mm^2)	0.165	0.158

Effective Prestress. The relationships between stress of PC strands and age are shown in Figure 5, in which the stress relaxation of PC strand is neglected. The stress of the PC strand on the top side in MS-U is smaller than that of Ref.-U. The difference of the stress between both beams after prestressing is not varied with age up to loading test and the difference is roughly close to that just before prestressing. The stress development before prestressing is induced by shrinkage, which may be affected by the difference of curing method at early ages between both beams. As for the stress of PC strand with age on the bottom side, the difference between both beams is small. The effective prestress of PC strands in Ref.-U and MS-U are shown in Table 4, which was calculated by Eq.(5).

$$f_p = \varepsilon_p E_p \quad (5)$$

where ε_p is the strain of PC strand from the time just before prestressing up to the time at loading test ; E_p is Young's modulus of PC strand.

As mentioned above, the stress loss due to relaxation in PC strand is neglected in the calculation of stress in Figure 5 and Table 4. As is summarized in the table, they are similar values when the effective ratios ($\gamma_{p\text{-}U}$, $\gamma_{p\text{-}L}$) of both PC beams are compared.

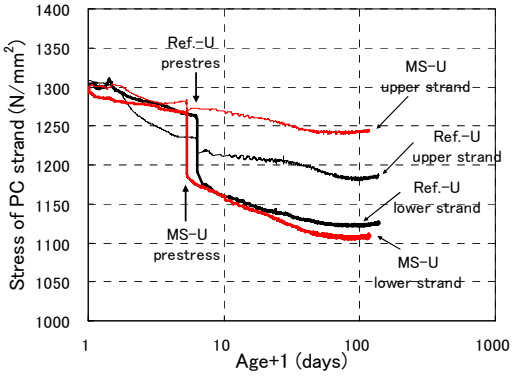

Figure 5. Stress of the PC strand calculated with the strain

Table 4. Effective prestress

Specimen				Ref.-U	MS-U
Top side PC strand	Initial prestress	$f_{p0\text{-}U}$	(N/mm^2)	1215	1270
	Change the strain	$\Delta\varepsilon_{p\text{-}U}$	(x10^{-6})	-163	-139
	Effective prestress	$f_{p\text{-}U}$	(N/mm^2)	1183	1244
	Effective ratio	$\gamma_{p\text{-}U}$		0.974	0.979
Bottom side PC strand	Initial prestress	$f_{p0\text{-}L}$	(N/mm^2)	1192	1180
	Change the strain	$\Delta\varepsilon_{p\text{-}L}$	(x10^{-6})	-344	-340
	Effective prestress	$f_{p\text{-}L}$	(N/mm^2)	1126	1114
	Effective ratio	$\gamma_{p\text{-}L}$		0.944	0.944

Cracking Pattern and Failure Mode. Flexural cracking forces ($V_{fck,exp}$), diagonal cracking forces ($V_{sck,exp}$) and shear force at failures ($V_{u,exp}$) are shown in Table 5. Shear strengths in the table are values of the half of the loading force. The flexural cracking force of MS-U is small about 8% compared with MS-U values. When load reached about 900kN (shear force 450kN), the flexural cracking started to occur also inclination which tended toward the load point with the increase in load. When load exceeded 1100kN (shear force 550kN), the diagonal crack prolonged from the beam lower end of the center of a shear span to about 100mm of lower part of the load point was occurred. The diagonal cracking load of MS-U has a smaller approximately 8% than the load of Ref.-U, and it was comparable with at the same level as decline ratio of the flexural cracking of MS-U. A decline of the tensile strength of the concrete is considered as a decline factor of the cracking load of MS-U. While deflections of the beam increased, after diagonal cracking, the load gradually increased and when compressive failure began to produce the beam upper edge of the concrete in the equivalent bending section, and the diagonal cracking reached the top and

Table 5. Strength of specimens

Shear Strength			Ref.-U	MS-U
Experimental result	Flexural cracking force	$V_{fck,exp}$	350	323
	Diagonal cracking force	$V_{sck,exp}$	602	555
	Shear force at failure	$V_{u,exp}$	622	632
Calcurated value	Flexual cracking force	$V_{fck,cal}$	249	246
	Flexual failure capacity	$V_{fu,cal}$	637	637
	Diagonal craking force	$V_{su,cal}$	225	212
		$V_{sck,exp}/V_{su,cal}$	2.68	2.61

bottom ends of the beam at a stretch and reached the fracture. The ultimate load of MS-U is at the same level as Ref.-U, and the influence that a replacement ratio of the molten slag fine aggregate gives to load capacity of UHSC in the range of 30% is small. Final crack patterns are shown in Figure 6. The diagonal cracks which had beams reach the fracture were 27-36 degrees for a horizontal axis. The upper section PC steel strands did buckling in the uniform bending moment section and those in the lower section did not failure.

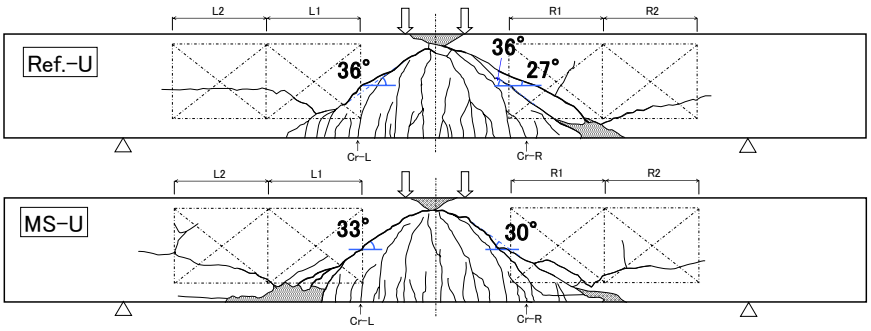

Figure 6. Crack patterns

Deflection. The relationship between load and the displacement of the mid-span is shown Figure 7. The deflection curves of both specimens overlap and show identical behavior. Flexural cracking is observed at an A point and does unloading once at a B point. Elastic behavior is shown in this extent. Flexural cracking has begun to occur at a C point within a shear span. The flexural cracking of the shear span began to progress while inclining to the diagonal direction, and MS-U was D point, and remarkable diagonal cracking produced Ref.-U in E point. The deflections of the beam increased afterwards, and Ref.-U and MS-U reached the fracture at an F point and a G point respectively. Shear displacement (S) was calculated from LVDTs set up in lateral face of the beam. In addition, the total displacement (T) of the measurement range was calculated by a gap of the vertical displacements of the both ends of this range, and the bending displacement (F) was calculated from the total displacement and difference with the shear displacement. The location of measurement of the shear displacements were four places in total, two places were in the right side (R1, R2) , another

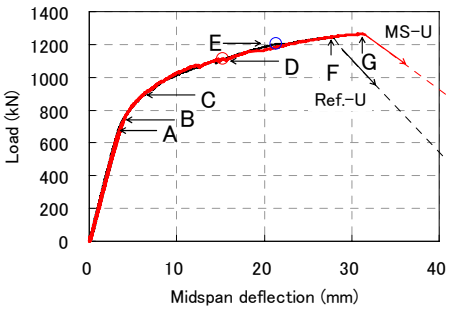

Figure 7. Load and deflection

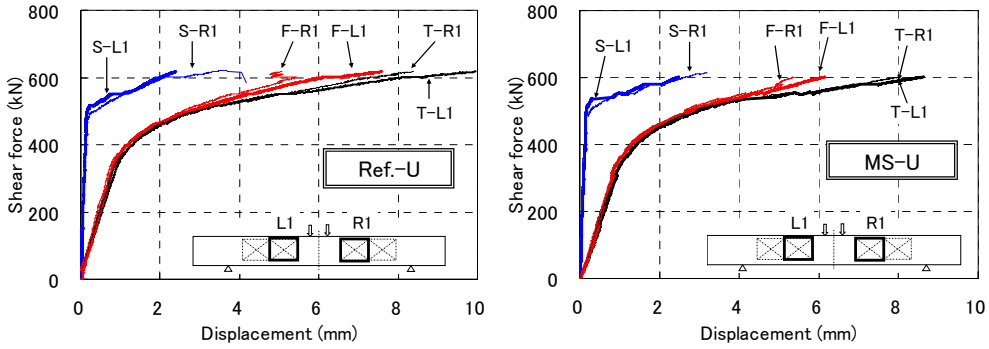

Figure 8. Shear Displacement

two places were in the left side (L1, L2) of the loading point. Total displacement, bending deflection and shear displacement and the relationship with the shear force are shown in Figure 8. Each displacement is shown in conventional sign of displacement component (S, T, F) and the location of measurement (L1, R1). The figures of L2 and R2 were omitted because cracks of these areas did not occur before failure of the beams. When the shear force was beyond about 500kN (load 1000kN), shear displacements of both beams increase. The behaviors scarcely change in L1 and R1. This depends on cracking of Cr-L shown in Figure 6 and cracking of Cr-R having occurred, respectively, in L1 and the R1 area.

Strain of the Concrete and the PC Strands. Compressive strain at the mid-span of the beam top surface is shown in Figure 9. The compressive strain in the fracture of both specimens reaches approximately 3500×10^{-6}. The distinction is not accepted by concrete compressive strain of both specimens. Strains of each sectional the lowest PC strand (mid-span (CL), loading point (L300, R300) and nearby center for the shear span (L1700, R1700)) and relationship of the load are shown in Figure 10. The PC strand strains were mean values of strain gages attached to diagonal wires, but adopted only one side when measurement inability occurs with the cracking growth. The PC steel strands of the constant moment zone shows value same as both beams. By the growth of the diagonal cracking which joined the loading point to the middle of the shear span, the PC strand strain of nearby middle of shear span increased and showed the strain at the same level as the constant moment zone. The strain of the bottom PC strand of the constant moment zone reaches the yield strain by a fracture. In addition, the yield strain depends on the material testing report.

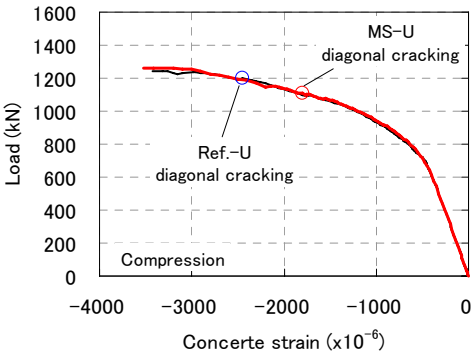

Figure 9. Load and concrete strain

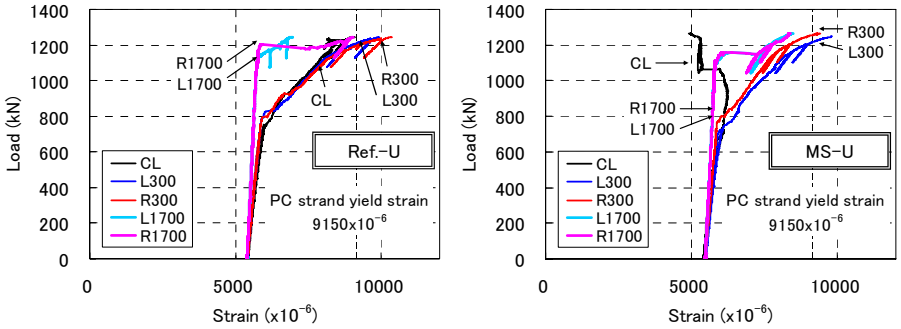

Figure 10. Load and strain of strands

Flexural Cracking. When tensile stress of the sum with compression stress by the prestress and the flexural cracking strength of the concrete acted, flexural cracking occurs, and calculated value ($V_{fck,cal}$) of concrete compressive strength less than $80N/mm^2$ is given in Eq. (6). Calculation result and measurement value are shown in Table 5. The measurement value of the flexural cracking was 1.3-1.4 times of the calculated value. Relationship with load and the biggest cracking width in a 1,000mm section of the mid-span which set up π shape displacements is shown in Figure 1.

$$V_{fck,cal} = \frac{W_p}{a}\left(f_{pe} + f_{bck}\right) \qquad (6)$$

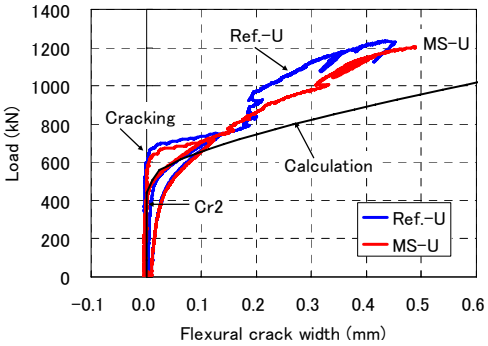

Figure 11. Maximum crack width

where W_p is the equivalent section modulus; f_{pe} is the stress by the prestress of the bottom of the concrete beam; $f_{bck}=k_{0b}k_{1b}f_{tk}$;k_{0b} is coefficient representing the relationship between tensile strength and flexural cracking strength on account of tension softening characteristics of concrete, $k_{ob}=1+1/\{0.85+4.5(h/l_{ch})\}$; k_{lb} is coefficient repressing reduction in strength on account of other reasons such as drying and heat of hydration, $k_{lb}=(0.55/h)^{1/4}$ ($\geqq 0.4$) ; h is the height of the beam; l_{ch} is the characteristic length, $l_{ch}=G_F E_c/f_t^2$; f_t is the tensile strength of the concrete; G_F is the fracture energy, it was used the value of Table 3; d_{max} is the maximum size of coarse aggregate (mm).

The flexural cracking width is given by Eq. (7). In the first loading, flexural cracking occurred in 650 - 700kN, and the cracking width was around 0.12mm. When unloading was done, the cracking width was almost closed, and the cracking opened again when loaded again. Measurement value of the cracking width accords with a calculated value to around 0.15mm well. Thereafter, progress of the flexural cracking which occurred within a shear span becomes remarkable, and enlargement of the cracking width in the loading span was restrained. Diagonal cracking strength calculation formula of the reinforced concrete beam which compressive strength does not use shear reinforcement for at 80-130N/mm^2 is suggested.

$$w = 1.1k_1k_2k_3\left\{4c + 0.7\left(c_s - \varphi\right)\right\}\frac{f_{pe}}{E_p} \qquad (7)$$

where k_1 is a constant to take into account the effect of surface geometry of reinforcement on crack width (in the case of PC strands, $k_1=1.3$); k_2 is a constant to take into account the effect of concrete quality on crack width, $k_2=15/(f'_c+20)+0.7$; k_3 is a constant to take into account the effect of multiple layers of PC strands on crack width, $k_3=5(n+2)/(7n+8)$; n is number of the layers of PC strands; c is concrete cover (mm); c_s is the center-to-center distance of PC strands (mm); φ is diameter of PC strands; and f_{pe} is increment of stress of PC strands from the state in which concrete stress at the portion of PC strands is zero(N/mm^2).

Failure Capacity. Diagonal cracking strength calculation formula of the high-strength reinforced concrete beam (compressive strength at 80-130N/mm^2) not to use shear reinforcement for was suggested by Sato, R. and Kawakane, H. (2008). Concept of the equivalence tension reinforcement ratio that tension reinforcement ratio decreases depending on shrinkage is used for the proposed equation in consideration of the influence that shrinkage of the concrete gives to shear strength. It was thought that the shrinkage of the concrete was reduced for a loss of the prestress, in these PC beams of this study, tension steel ratio (p_s) was used. The influence that prestress gave in shear capacity by method to multiply

member using decompression moment (M_0) provided in JSCE standard specifications (2007) by proposed equation were considered. In calculation of M_0, it was calculated using effective prestress from the strain of PC strands to show in Table 4. Diagonal cracking load calculation formula in consideration of term (β_n) representing influence of the axial force in proposed equation is shown in Eq.(9). The shear capacity that the coverage of the proposed equation was expanded to 150N/mm^2 was calculated is shown in Table 5 as $V_{su,cal}$. The experimental diagonal cracking force ($V_{sck,exp}$) of MS-U was 555kN, whereas the calculated diagonal cracking force ($V_{su,cal}$) was 212kN. The diagonal cracking load had strength more than 2.6 times of value calculated in proposed equation.

$$V_{su} = 0.206\left(E_c G_F\right)^{2/5} f_t^{1/5} \left(100 p_s\right)^{1/3} d^{-2/5} \left(0.75 + 1.4/\left(a/d\right)\right) b_w d \beta_n \quad (9)$$

where b_w is web width; d is effective depth; p_s is the tension PC strand ratio; $\beta_n = 1 + 2M_0/M_d$; M_d is pure flexural capacity without consideration of axial force; and M_0 is decompression moment.

CONCLUSIONS

Based on the test program to investigate the effect of Molten Slag fine aggregate on the shear behaviour of prestressed ultra high strength concrete beams, the following conclusions are drawn:

1. UHSC containing the molten slag with the replacement ratio of 30% in volume as fine aggregate (MS-U), reached 150 N/mm^2 in compressive which was the same as that of UHSC not containing the molten slag (Ref.-U). Young's Modulus of the former was also equal to that of the latter.

2. The mechanical performance of the pretentioned MS-U beam was completely equivalent to that of reference Ref.-U beam except for the cracking force.

3. The diagonal cracking force of the MS-U beam was slightly smaller than that of the Ref.-U beam. The cause may be due to slightly small tensile strength of MS-U compared with that of Ref.-U.

REFERENCES

Japan Concrete Institute (JCI) (2001). "Method of test for fracture energy of concrete by use of notched beam", Technical report on test method of concrete fracture, pp.401-426.

Japan Society of Civil Engineers (JSCE) (2007). Standard Specifications for Concrete Structures "Design", JSCE, Guidelines for Concrete No.15

Japan Prestressed Concrete Engineering Association (PCEA) (2008). Guidelines for Design and Construction of High-strength Concrete for Prestressed Concrete Structures, pp28-29.

Kawakane, H. and Sato, R. (2009). "Evaluation of Shrinkage Effects on Diagonal Cracing Strength of Reinforced HSC beams", Journal of JSCE, Vol.65, No.2, pp.178-197.

Sato, R. and Kawakane, H. (2008). "A new concept for the early age shrinkage effect on diagonal cracking strength of reinforced HSC beams", journal of Advanced Concrete Technology, Vol.6, No.1, pp.45-67.